

---

# END-TO-END 3D SPATIOTEMPORAL PERCEPTION WITH MULTIMODAL FUSION AND V2X COLLABORATION

---

**Zhenwei Yang**

National Center for Materials Service Safety  
 University of Science and Technology Beijing  
 Beijing 100083, China  
 d202110534@xs.ustb.edu.cn

**Yibo Ai**

National Center for Materials Service Safety  
 University of Science and Technology Beijing  
 Beijing 100083, China  
 ybai@ustb.edu.cn

**Weidong Zhang**

National Center for Materials Service Safety  
 University of Science and Technology Beijing  
 Beijing 100083, China  
 wdzhang@ustb.edu.cn

December 29, 2025

## ABSTRACT

Multi-view cooperative perception and multimodal fusion are essential for reliable 3D spatiotemporal understanding in autonomous driving, especially under occlusions, limited viewpoints, and communication delays in V2X scenarios. This paper proposes XET-V2X, a multi-modal fused end-to-end tracking framework for v2x collaboration that unifies multi-view multimodal sensing within a shared spatiotemporal representation. To efficiently align heterogeneous viewpoints and modalities, XET-V2X introduces a dual-layer spatial cross-attention module based on multi-scale deformable attention. Multi-view image features are first aggregated to enhance semantic consistency, followed by point cloud fusion guided by the updated spatial queries, enabling effective cross-modal interaction while reducing computational overhead. Experiments on the real-world V2X-Seq-SPD dataset and the simulated V2X-Sim-V2V and V2X-Sim-V2I benchmarks demonstrate consistent improvements in detection and tracking performance under varying communication delays. Both quantitative results and qualitative visualizations indicate that XET-V2X achieves robust and temporally stable perception in complex traffic scenarios.

**Keywords** Multimodal Fusion · Multi-view Cooperative Perception · Spatiotemporal Modeling · V2X Communication

## 1 Introduction

3D spatiotemporal perception has become a foundational capability for intelligent systems as advances in artificial intelligence, IoT infrastructures, and multi-source sensing continue to reshape autonomous perception. By jointly modeling spatial structure and temporal evolution, 3D spatiotemporal perception enables continuous understanding of object geometry, motion trajectories, and behavioral patterns. This paradigm has proven essential for autonomous driving, where safety-critical applications such as 3D detection, multi-object tracking, trajectory forecasting, and motion planning require reliable scene representations over time.

A large body of prior research has explored improvements in both spatial and temporal aspects of perception. Single-vehicle systems that fuse data from cameras, LiDAR, and inertial sensors have demonstrated strong performance in static reconstruction, dynamic obstacle detection, and sequential prediction. Meanwhile, temporal fusion techniques—particularly Transformer-based BEV models—have significantly enhanced multi-frame detection stability, cross-frame feature alignment, and long-term trajectory reasoning. Beyond single-agent sensing, multi-view cooperative

perception in V2X scenarios has emerged as a complementary strategy to overcome occlusions and restricted fields of view. By exchanging raw sensor observations, intermediate features, or high-level perceptual results across vehicles and roadside units, cooperative systems have achieved extended perception range and more reliable detection of hidden objects. Representative studies include cooperative LiDAR perception [1, 2], communication-efficient feature sharing [3, 4], and large-scale benchmarks such as DAIR-V2X[5], V2X-Sim[6], and V2V4Real [5, 6, 7], which have accelerated progress in collaborative perception research.

Despite these advances, several limitations remain. Single-vehicle perception still suffers from view occlusion, blind spots, and geometric distortions that hinder reliable understanding in dense urban environments. Existing cooperative approaches often rely on modular, stage-wise pipelines—such as separate detection, temporal matching, fusion, and tracking—which introduce redundant computation and accumulate errors across steps. Moreover, most V2X research focuses on either spatial fusion or modality fusion but rarely integrates temporal modeling into a unified cross-agent framework. Heterogeneous sensors across agents further complicate cross-view geometric alignment, spatiotemporal synchronization, and feature consistency, particularly under communication constraints or domain shifts. These challenges collectively restrict the robustness, continuity, and scalability of current 3D spatiotemporal perception systems.

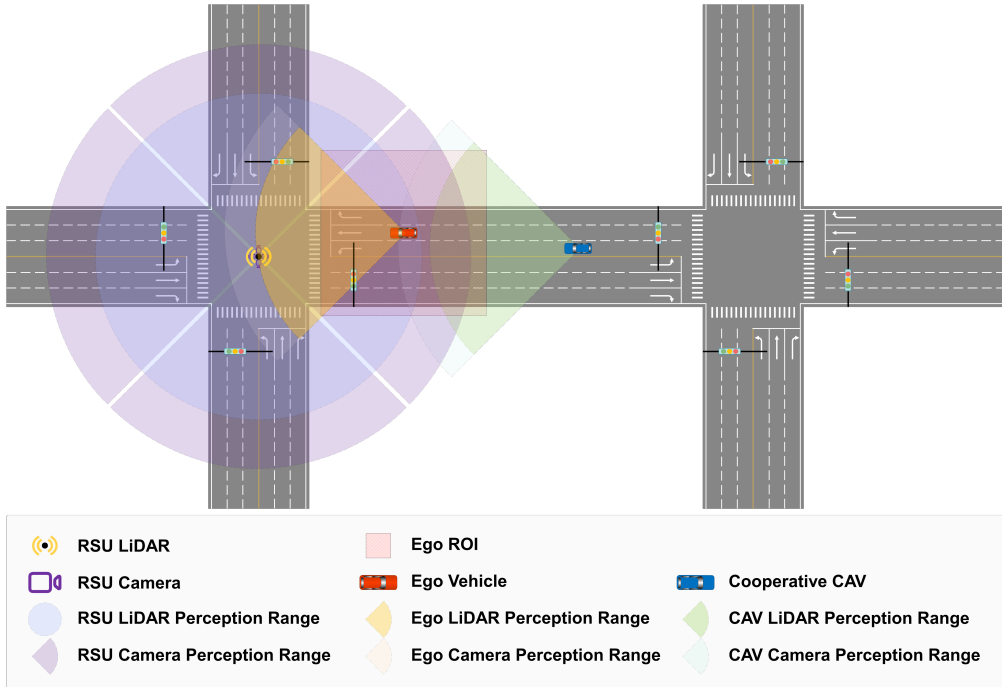


Figure 1: **V2X Cooperative Perception Diagram.** The red vehicle denotes the ego vehicle, while the blue vehicles represent cooperative CAVs. Both the ego vehicle and cooperative CAVs are equipped with forward-facing fan-shaped cameras and LiDAR sensors with front-view coverage. The RSU is equipped with fan-shaped cameras covering the four approaches of the intersection and a 360° LiDAR sensor, providing comprehensive infrastructure-side perception.

To address these gaps, this study presents a unified end-to-end framework that integrates multi-view collaboration, multi-modality fusion, and temporal modeling within a single learnable architecture, as illustrated in Fig. 1. By jointly exploiting complementary geometric cues from distributed LiDARs and semantic information from multiple cameras, the proposed framework establishes a shared BEV representation that supports cross-view consistency and long-horizon motion reasoning. A dual-layer cross-modal and cross-view attention mechanism enables fine-grained interaction between heterogeneous features, while Transformer-based temporal encoding captures long-term trajectories and mitigates occlusion-induced discontinuities. Extensive experiments on the V2X-Seq-SPD [5] and V2X-Sim [6] datasets demonstrate substantial improvements in both detection and tracking performance over single-view or single-modality baselines.

The contributions are summarized as follows:

- We propose a unified end-to-end 3D spatiotemporal perception framework that jointly integrates multi-view collaboration, multi-modality fusion, and temporal modeling within a single optimization process.

- We design a dual-layer cross-modal-cross-view interaction module and a shared BEV representation that achieve robust geometric alignment and information completion across distributed agents.
- We demonstrate state-of-the-art performance on large-scale V2X benchmarks, showing significant gains in long-range detection, occlusion handling, and multi-object tracking stability.

The remainder of this paper is organized as follows. Section II reviews the related works relevant to this study. In Section III, we present XET-V2X, our proposed multi-modal fused end-to-end tracking framework for V2X Collaboration. Section IV details the experimental results and analysis. Finally, Section V concludes the paper.

## 2 Related Works

### 2.1 Multi-View Cooperative Perception

Multi-view cooperative perception in V2X scenarios aims to aggregate observations from multiple spatially distributed agents, including CAVs and RSUs, to achieve a more complete and robust understanding of the environment. Unlike ego-centric surround-view perception based on on-board multi-camera systems, V2X-based cooperative perception explicitly exploits complementary viewpoints across different platforms, enabling extended perception range and reduced occlusion.

Early studies focused on cooperative warning and shared sensing frameworks [8, 9], demonstrating the potential of inter-vehicle information exchange. Subsequent works investigated cooperative 3D perception using raw sensor sharing, intermediate feature fusion, or decision-level fusion. Representative approaches include multi-vehicle LiDAR-based 3D detection and tracking through point cloud sharing and feature collaboration [1, 2], as well as neural communication frameworks such as V2VNet [3] and communication-efficient designs like Where2Comm [4]. These methods validate the effectiveness of collaborative perception under limited communication budgets.

The release of large-scale cooperative perception benchmarks, such as LET-VIC [10], DAIR-V2X [11], OpenV2V [12], and V2V4Real [7], has further accelerated research in this field. Despite recent progress, most existing approaches remain modular and task-oriented, and often lack unified temporal modeling and end-to-end optimization across agents and time, limiting their scalability in dynamic real-world driving environments.

### 2.2 Multimodal Fusion Perception

Multimodal 3D object detection exploits complementary cues from heterogeneous sensors such as cameras, LiDAR, and radar. Existing approaches are typically categorized into early fusion, intermediate fusion, and late fusion. Early fusion methods inject image-derived semantic or geometric information into point clouds prior to LiDAR-based detection, as exemplified by PointPainting [13] and related approaches. Intermediate fusion methods perform deeper feature interaction across modalities, addressing alignment challenges via attention mechanisms, deformable sampling, or Transformer-based architectures [14, 15, 16]. Recent works such as TransFusion [17], FUTR3D [18], and DeepInteraction [19] formulate multimodal fusion as a unified, end-to-end learning problem using query-based Transformers.

Late fusion strategies combine independent detection results from different modalities, offering robustness and modularity but limited cross-modal interaction. Overall, although multimodal fusion significantly improves perception reliability, effectively aligning heterogeneous representations across sensors and viewpoints remains a fundamental challenge.

### 2.3 Temporal Information Fusion

Temporal fusion exploits correlations across consecutive frames to enhance perception stability, especially under motion and occlusion. Prior works incorporate temporal context using sequential aggregation or recurrent mechanisms [20]. For BEV-based multi-view perception, RecurrentBEV [21] introduces recurrent feature updates to preserve long-term temporal information. In cooperative perception settings, recent studies such as V2XPnP [22] explore joint spatiotemporal fusion across vehicles and time. With the rise of Transformer-based spatiotemporal modeling, temporal fusion has become an essential component for robust detection and tracking in dynamic environments.

### 2.4 End-to-End Multi-Object Tracking

End-to-end perception frameworks aim to unify detection and tracking within a single network. Vision-based methods such as CenterTrack [23] and TrackFormer [24] integrate detection and data association through unified representations

and track queries. MOTR [25] further extends this paradigm by iteratively updating track queries across frames. For point cloud and multimodal tracking, recent Transformer-based frameworks jointly reason over spatial and temporal features [26, 27]. By removing explicit post-hoc association steps, end-to-end tracking simplifies the pipeline and improves identity consistency.

## 2.5 Difference from Our Work

Despite significant progress in multi-view perception, multimodal fusion, cooperative sensing, and end-to-end tracking, most existing methods address these aspects in isolation. Multi-camera 3D detection primarily focuses on single-vehicle perception, while cooperative perception systems often rely on modular pipelines and limited temporal modeling. Similarly, multimodal fusion and end-to-end tracking are typically designed for standalone agents, without explicitly considering V2X collaboration under dynamic spatiotemporal conditions.

In contrast, our work presents an *end-to-end 3D spatiotemporal perception framework* that tightly integrates **multi-view visual perception, multimodal sensor fusion, and V2X-based collaboration** within a unified learning paradigm. By jointly modeling spatial geometry, temporal evolution, and cross-agent information exchange, the proposed approach enables consistent perception across vehicles and time, offering a scalable and practical solution for connected autonomous driving scenarios.

## 3 Method

This section presents the proposed multi-view cooperative spatiotemporal perception model with multimodal fusion, termed **XET-V2X**. Building upon an end-to-end 3D temporal perception framework, XET-V2X integrates a multi-view cooperative mechanism to dynamically fuse multimodal sensor data collected from the ego vehicle and other cooperative agents. This design explicitly addresses practical challenges such as sensor calibration errors, limited representational capacity of single-modality sensors, and restricted field of view of individual sensing agents. By jointly exploiting multi-view, multimodal, and temporal information, XET-V2X achieves more accurate object detection and tracking, thereby enhancing environmental perception and enabling safer and more efficient autonomous driving.

### 3.1 Task Formulation

This work addresses a *V2X-based multi-view cooperative spatiotemporal perception* task for autonomous driving, where the ego vehicle collaborates with other agents, such as roadside units (RSUs) and connected and automated Vehicles (CAVs), to perform 3D object detection and tracking using temporally ordered multimodal sensor data. Each agent is equipped with heterogeneous sensors, including cameras and LiDARs, providing complementary geometric and semantic observations from diverse viewpoints.

Unlike single-vehicle perception, cooperative perception explicitly exploits spatial complementarity and temporal continuity across distributed sensing agents. By sharing perception-relevant information through V2X communication, the system aims to mitigate occlusion, extend perception range, and enhance spatiotemporal consistency of object states in complex traffic environments.

**Temporal Modeling and Notation** After preprocessing, sensor observations from the ego vehicle and other cooperative agents are organized into a temporal sequence of length  $N$ , indexed by  $k = 1, 2, \dots, N$ . Let  $t_{\text{ego},k}$  and  $t_{\text{other},k}$  denote the acquisition times of the ego-view and other-view observations at index  $k$ , respectively. The temporal indices satisfy a strictly increasing order for each agent, while  $t_{\text{other},k} \leq t_{\text{ego},k}$  holds due to communication latency in V2X transmission.

We assume that each agent internally synchronizes its onboard sensors (e.g., camera and LiDAR), ensuring that multimodal data collected by the same agent at index  $k$  correspond to the same timestamp. This assumption is consistent with practical vehicular and RSU sensing systems, and does not require strict inter-agent time alignment.

**Input Representation** At time index  $k$ , the cooperative perception system receives:

- Ego-view multimodal observations  $(S_{\text{ego},k}^{\text{pc}}, S_{\text{ego},k}^{\text{img}})$ , together with the corresponding calibration parameters  $(M_{\text{ego},k}^{\text{pc}}, M_{\text{ego},k}^{\text{img}})$ ;
- Multimodal observations from other cooperative agents  $(S_{\text{other},k}^{\text{pc}}, S_{\text{other},k}^{\text{img}})$ , with calibration parameters  $(M_{\text{other},k}^{\text{pc}}, M_{\text{other},k}^{\text{img}})$ , transmitted to the ego vehicle via V2X communication.

These observations jointly encode geometric structure and semantic appearance from multiple viewpoints over time, forming the basis for cooperative spatiotemporal perception.

**Output Definition** At ego time  $t_{\text{ego},k}$ , the system outputs a set of detected and tracked objects:

$$\mathcal{O}_k = \left\{ (c_{i,k}, p_{i,k}, d_{i,k}, \theta_{i,k}, \mathcal{T}_i) \right\}_{i=1}^{\mathcal{D}_k}, \quad (1)$$

where  $c_{i,k}$  denotes the object category,  $p_{i,k}$  its 3D position,  $d_{i,k}$  its 3D dimensions,  $\theta_{i,k}$  its orientation, and  $\mathcal{T}_i$  a persistent tracking identity.  $\mathcal{D}_k$  denotes the number of objects perceived at time  $k$ .

**Ground Truth and Training Objective** The ground truth at time  $t_{\text{ego},k}$  aggregates annotations from all cooperative agents and sensing modalities, restricted to the ego-centric region of interest  $\text{ROI}_{\text{ego},k}$ :

$$\text{GT}_k = \left( \text{GT}_{\text{ego},k}^{\text{pc}} \cup \text{GT}_{\text{ego},k}^{\text{img}} \cup \text{GT}_{\text{other},k}^{\text{pc}} \cup \text{GT}_{\text{other},k}^{\text{img}} \right) \cap \text{ROI}_{\text{ego},k}, \quad (2)$$

which can be equivalently represented as

$$\text{GT}_k = \left\{ (c_{i,k}, p_{i,k}, d_{i,k}, \theta_{i,k}, \mathcal{T}_i) \right\}_{i=1}^{\mathcal{G}_k}, \quad (3)$$

where  $\mathcal{G}_k$  is the number of ground-truth objects at time  $k$ .

Based on  $\{\mathcal{O}_k\}_{k=1}^N$  and  $\{\text{GT}_k\}_{k=1}^N$ , the cooperative perception task jointly optimizes detection accuracy, localization precision, and temporal identity consistency under multi-view and multi-agent settings.

### 3.2 Motivation and Design Rationale for Multi-View Cooperative Multimodal Fusion

As formulated in the previous section, V2X-based cooperative spatiotemporal perception aims to jointly perform 3D object detection and tracking by leveraging temporally ordered multimodal observations from distributed sensing agents. Compared with single-vehicle perception, this task introduces two fundamental challenges: (i) how to effectively exploit spatial complementarity across heterogeneous viewpoints, and (ii) how to maintain consistent object representations over time in the presence of communication latency and sensing uncertainty.

From a spatial perspective, perception from a single viewpoint is inherently limited by occlusion, restricted field of view, and range constraints. Even with multi-camera or LiDAR-camera setups onboard a single vehicle, blind spots and long-range perception degradation remain unavoidable, especially in complex traffic scenarios such as intersections and dense urban environments. V2X-based multi-view collaboration enables the ego vehicle to incorporate complementary observations from RSUs and CAVs, thereby extending perception coverage and alleviating occlusions through viewpoint diversity. This spatial redundancy forms the basis for more complete and reliable 3D scene understanding.

From a modal perspective, LiDAR and camera sensors exhibit fundamentally different yet complementary characteristics. LiDAR provides accurate 3D geometry and depth measurements, which are critical for precise localization and size estimation, while cameras capture rich appearance, texture, and semantic cues that facilitate object classification and attribute recognition. Relying on a single modality leads to inherent vulnerabilities under adverse lighting or weather conditions. By fusing LiDAR and camera data across multiple cooperative agents, the perception system gains robustness against modality-specific degradation, making it more suitable for real-world autonomous driving scenarios.

From a temporal perspective, object detection and tracking are intrinsically dynamic tasks. Isolated frame-wise perception is insufficient for ensuring identity consistency, motion continuity, and stable state estimation. Temporal modeling allows the system to exploit motion patterns, smooth noisy observations, and associate objects across time under asynchronous data arrival in V2X communication. Importantly, cooperative temporal fusion does not require strict inter-agent synchronization; instead, it can flexibly accommodate bounded communication delays while preserving spatiotemporal consistency at the ego vehicle.

Based on these considerations, this work adopts a multi-view cooperative multimodal fusion paradigm, in which temporally ordered LiDAR and camera observations from the ego vehicle and other V2X agents are jointly modeled. The design explicitly integrates spatial complementarity, modality diversity, and temporal continuity, forming a unified perception framework that addresses the core limitations of single-view, single-modality, and frame-centric approaches. This motivation directly guides the architectural choices presented in the following sections.

### 3.3 Model Architecture

The overall architecture of XET-V2X is illustrated in Fig. 2. The core design of the model lies in multi-view multimodal feature extraction and multi-view multimodal feature fusion. For both the ego view and other cooperative views

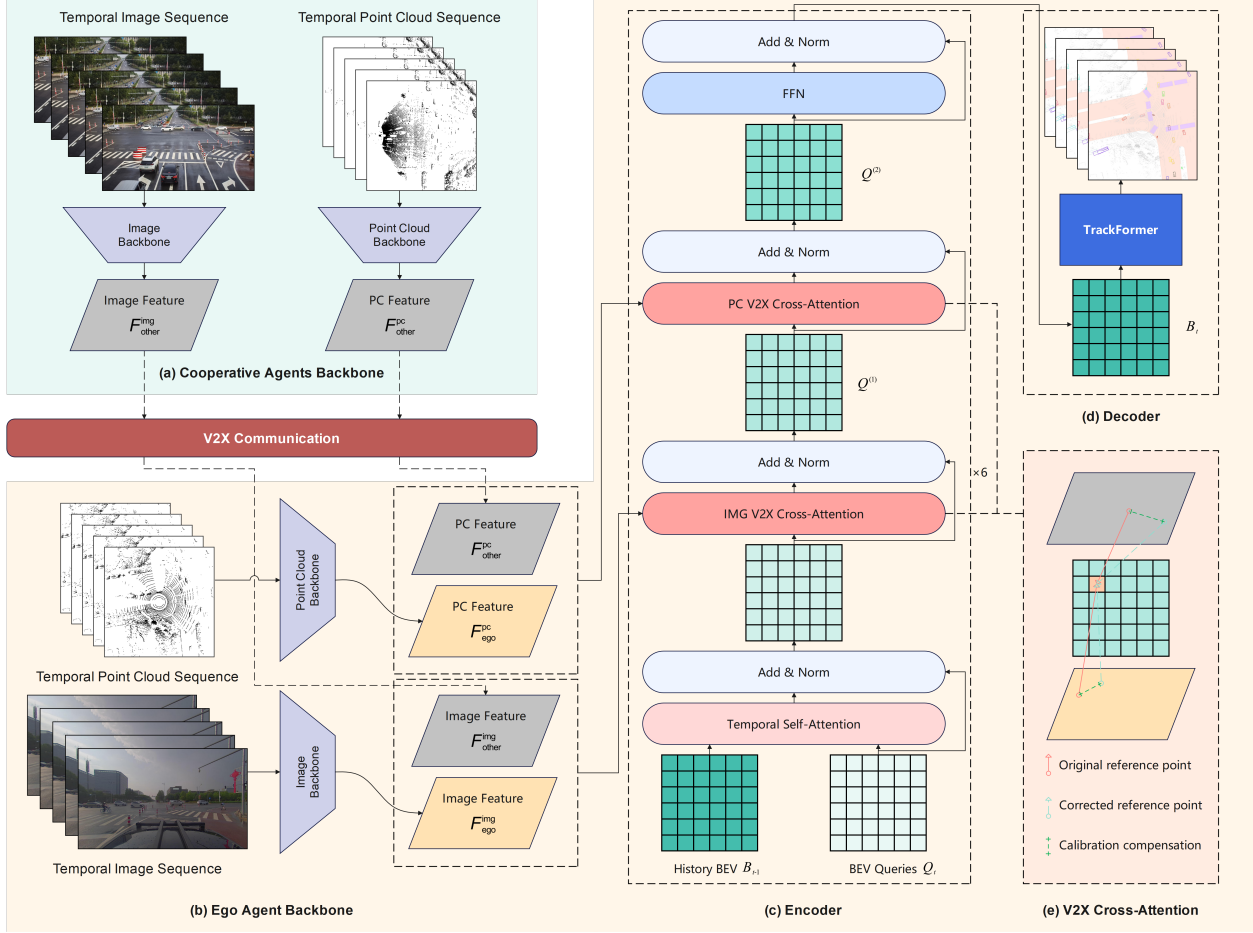


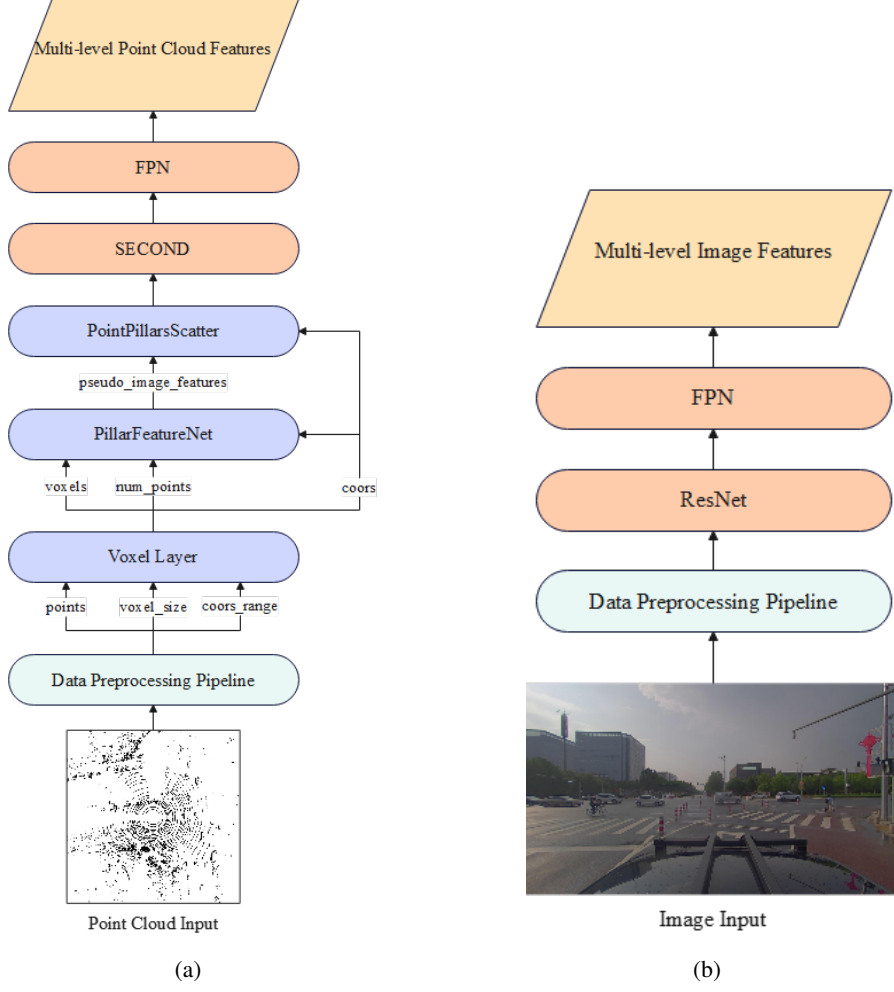
Figure 2: Architecture of XET-V2X

(i.e., RSUs or CAVs), XET-V2X employs PointPillars [28] to extract point cloud features and ResNet [29] to extract image features, yielding high-dimensional feature representations. Subsequently, two stacked multi-view cooperative cross-attention modules are applied to fuse features across viewpoints and modalities. Finally, object detection and tracking are performed based on the MOTR framework [25], enabling joint detection and tracking in an end-to-end manner.

### 3.4 Multi-View Multimodal Feature Extraction

**Multi-View Point Cloud Feature Extraction** Fig. 3a illustrates the point cloud feature encoding backbone for the ego vehicle and cooperative agents in the XET-V2X framework, corresponding to the architectures shown in Fig. 2 (a) and (b). This backbone adopts a hierarchical feature encoding pipeline that transforms raw point clouds into multi-scale BEV feature representations. Specifically, raw point cloud data are first preprocessed and then voxelized into a regular 3D grid structure. A pillar-based feature encoding module (PillarFeatureNet) is subsequently employed to project 3D point cloud information into a 2D BEV pseudo-image representation. Finally, cascaded sparse convolutional networks (SECOND) and a Feature Pyramid Network (FPN) are applied to perform multi-scale feature aggregation and enhancement, constructing a hierarchical feature pyramid with varying receptive fields to improve perception across objects of different sizes.

In this work, efficient point cloud processing is implemented based on the PointPillars framework [28], which significantly reduces computational complexity while preserving essential 3D geometric information through pillar-wise partitioning (pillar size:  $0.2 \text{ m} \times 0.2 \text{ m} \times 8 \text{ m}$ ). As illustrated in the processing pipeline, the raw 3D point cloud ( $x, y, z$ ) is first preprocessed, followed by voxelization within modality-specific regions of interest (ROI) defined according to sensor placement:

Figure 3: **Backbone.** (a) Point Cloud Backbone; (b) Image Backbone.

- Ego-vehicle ROI in the V2X-Seq-SPD dataset [5]:  $x \in [-51.2, 51.2]$  m,  $y \in [-51.2, 51.2]$  m,  $z \in [-5.0, 3.0]$  m;
- Roadside ROI in the V2X-Seq-SPD dataset [5]:  $x \in [0, 102.4]$  m,  $y \in [-51.2, 51.2]$  m,  $z \in [-5.0, 3.0]$  m;
- Ego-vehicle ROI in the V2X-Sim dataset [6]:  $x \in [-51.2, 51.2]$  m,  $y \in [-51.2, 51.2]$  m,  $z \in [-3.0, 5.0]$  m;
- Other-agent ROI in the V2X-Sim dataset [6]:  $x \in [-51.2, 51.2]$  m,  $y \in [-51.2, 51.2]$  m,  $z \in [-3.0, 5.0]$  m.

The voxel size is set to 0.2 m along the  $x$  and  $y$  axes and 8 m along the  $z$  axis. Accordingly, both ego-view and other-view BEV grids have a spatial resolution of  $512 \times 512$ . Each voxel stores the points falling within it along with their corresponding coordinate information.

During feature encoding, PillarFeatureNet employs multi-layer perceptrons (MLPs) to encode geometric features, transforming unstructured point cloud data into structured 2D BEV pseudo-image feature maps. The PointPillarsScatter module distributes sparse features into dense grid space via an unpooling operation, after which sparse convolution layers in the SECOND network further refine the features. Submanifold convolutions are adopted to effectively suppress redundant computation on empty voxels. Finally, the Feature Pyramid Network (FPN) performs top-down fusion with lateral connections to produce a three-level feature pyramid  $\{P2, P3, P4\}$ , corresponding to perception resolutions of 0.4 m, 0.8 m, and 1.6 m, respectively. This design achieves a balance between computational efficiency and multi-scale perception capability.

**Multi-View Image Feature Extraction** Fig. 3b shows the image feature encoding backbone for both vehicle-mounted and roadside cameras in the XET-VIC framework, corresponding to the architectures illustrated in Fig. 2 (a) and (b).

This backbone follows a hierarchical feature encoding paradigm that converts raw images into multi-scale feature representations. Specifically, input images are first subjected to standard preprocessing and augmentation operations, including resizing, normalization, and padding. A Residual Network (ResNet) is then employed to extract feature maps at different semantic levels. Subsequently, a Feature Pyramid Network (FPN) fuses multi-level features through top-down pathways and lateral connections, generating a set of multi-scale image features with unified channel dimensions and varying spatial resolutions to improve detection of objects at different scales.

In XET-VIC, the image backbone is built upon the ResNet-101 architecture [29], with multi-scale feature fusion realized via a FPN. During preprocessing, all input images are resized, normalized, and padded to match the network input requirements. The ResNet-101 backbone consists of four residual stages, from which feature maps C2, C3, and C4 (with channel dimensions of 512, 1024, and 2048, respectively) are extracted from the second, third, and fourth stages. Deformable convolutions (DCNv2) are incorporated into the conv4\_x and conv5\_x stages to enhance robustness to geometric deformations, while the remaining layers are frozen to stabilize training. The FPN module subsequently performs top-down channel mapping and spatial interpolation with lateral connections, producing four pyramid levels  $\{P_2, P_3, P_4, P_5\}$  with unified channel dimensions. These multi-scale features provide rich representations ranging from fine-grained to coarse-level semantics for downstream detection and segmentation heads, effectively improving performance on objects of varying sizes while maintaining computational efficiency.

### 3.5 Multi-View Image Feature Transmission in XET-V2X

To support cooperative perception under practical V2X communication constraints, XET-V2X adopts feature-level image transmission as the primary information exchange paradigm among distributed perception agents. As illustrated between Fig. 2 (a) and (b), image features extracted at remote agents (e.g., infrastructure or other connected vehicles) are transmitted to the ego vehicle for subsequent cooperative fusion.

In V2X systems, transmissible information can be broadly categorized into three levels: raw sensor data, instance-level perception results, and feature-level intermediate representations. These three forms exhibit distinct trade-offs between communication bandwidth and information preservation [30, 31]. Raw sensor data, such as uncompressed images or video streams, preserve complete scene information but incur prohibitive bandwidth requirements. Instance-level perception results, including detected bounding boxes, categories, and attributes, achieve minimal communication cost at the expense of severe information loss. Feature-level intermediate representations, extracted by deep neural networks, offer a favorable balance by retaining rich semantic and structural information while significantly reducing transmission overhead [31].

Motivated by the above considerations, XET-V2X prioritizes image feature transmission for cooperative perception. First, feature-level representations enable substantial bandwidth savings—typically several to tens of times smaller than raw images—making them suitable for latency- and bandwidth-constrained V2X links. Second, compared to instance-level results, image features preserve global contextual cues and fine-grained spatial structures, which are critical for high-level perception tasks under occlusion and long-range scenarios. Third, feature transmission naturally supports cross-view alignment and fusion at the ego vehicle, where collaborative perception is realized through a multi-view cross-attention mechanism, allowing complementary information from heterogeneous viewpoints to be effectively integrated.

By transmitting image features and deferring multi-view interaction to the ego vehicle, XET-V2X achieves efficient information sharing while maintaining strong cooperative perception capability, thereby aligning with the task formulation of distributed yet coordinated V2X perception.

### 3.6 Multi-View Multimodal Feature Transmission

Fig. 2 (a) and (b) illustrate the process of transmitting point cloud and image features from cooperative agents to the ego vehicle. In V2X communication, transmissible information can generally be categorized into three types: raw sensor data, instance-level perception results, and feature-level intermediate representations. The proposed XET-V2X framework prioritizes the transmission of point cloud and image features. By favoring image feature transmission and combining it with a multi-view cooperative cross-attention mechanism, the framework effectively reduces V2X communication bandwidth requirements while preserving critical perception performance, thereby enabling efficient feature sharing and fusion in multi-view cooperative scenarios.

### 3.7 Multi-View Multimodal Feature Fusion

Conventional multi-view feature fusion methods face two major challenges. First, dense global attention over high-dimensional features incurs substantial computational overhead. Second, spatial calibration discrepancies across

heterogeneous viewpoints and sensing modalities lead to feature misalignment, which degrades fusion effectiveness. These challenges are further amplified in V2X scenarios, where observations originate from multiple agents and multiple sensing modalities. To address these issues, the proposed XET-V2X framework introduces a dual-layer spatial cross-attention module based on multi-scale deformable attention, enabling efficient and robust multi-view multimodal feature fusion.

Given a set of BEV queries  $Q^{bev}$ , the proposed *V2X Cross-Attention* aggregates features from the ego agent and other cooperative agents. Each agent provides multi-modal features, including image features and point cloud features. Formally, the V2X Cross-Attention is defined as:

$$\text{V2XCrossAttn}(Q^{bev}, F^{ego}, F^{other}, P^{ego}, P^{other}) = \sum_{i=1}^{N_{ref}} \left[ \frac{1}{1 + \mathcal{M}_i^{other}} \left( \text{MSDeformAttn}(Q_i^{bev}, P_i^{ego}, F^{ego}) \right. \right. \\ \left. \left. + \mathcal{M}_i^{other} \cdot \text{MSDeformAttn}(Q_i^{bev}, P_i^{other}, F^{other}) \right) \right], \quad (4)$$

where  $i$  indexes the BEV reference points and  $N_{ref}$  denotes the total number of reference points.  $F^{ego}$  and  $F^{other}$  represent the multi-modal feature sets from the ego agent and other cooperative agents, respectively, each consisting of image and point cloud features.  $P_i^{ego}$  and  $P_i^{other}$  are the normalized coordinates of the  $i$ -th reference point projected onto the corresponding BEV feature spaces.  $\mathcal{M}_i^{other}$  is a validity mask that excludes reference points falling outside the spatial support of the other agents' features.

The core operation in Eq. 4 is the multi-scale deformable attention (MSDeformAttn), which efficiently aggregates sparse local features across multiple scales. It is formulated as:

$$\text{MSDeformAttn}(Q_i, P_i, \{F^l\}_{l=1}^L) = \sum_{m=1}^M W_m \left[ \sum_{l=1}^L \sum_{k=1}^K A_{mlqk} \cdot W_m' F_i^l (\mathcal{R}_l(P_i) + \Delta p_{mlqk}) \right], \quad (5)$$

where  $m$  indexes the attention heads,  $l$  indexes the feature levels, and  $k$  indexes the sampling points.  $\Delta p_{mlqk}$  and  $A_{mlqk}$  denote the learnable sampling offsets and normalized attention weights, respectively. This formulation allows the attention mechanism to adaptively focus on informative regions while compensating for spatial misalignment, achieving both efficiency and robustness.

As illustrated in Fig. 2 (c) and (e), the proposed multi-view multimodal fusion is implemented through two cascaded spatial cross-attention layers. The first layer performs multi-view fusion within the image modality, aligning and aggregating visual semantics from different viewpoints to construct an image-enhanced BEV representation. The second layer subsequently fuses point cloud features under the guidance of the updated BEV queries, thereby enabling explicit cross-modal interaction and enforcing spatial consistency between image and LiDAR modalities. This progressive fusion process can be expressed as:

$$Q^{(1)} = \text{V2XCrossAttn}(Q^{bev}, F_{img}^{ego}, F_{img}^{other}), \quad Q^{(2)} = \text{V2XCrossAttn}(Q^{(1)}, F_{lidar}^{ego}, F_{lidar}^{other}), \quad (6)$$

where  $Q^{(2)}$  serves as the final multi-view multimodal BEV representation.

Experimental results show that the *image-first, point-cloud-second* fusion order consistently achieves slightly better performance across all datasets, while the reverse order remains competitive. This indicates that the proposed framework is robust to fusion order variations. Accordingly, the image-first fusion strategy is adopted as the default configuration in this study.

Overall, the proposed dual-layer deformable cross-attention module enables deep integration of multi-view and multimodal information within a unified and computationally efficient framework, providing robust BEV features for end-to-end 3D spatiotemporal perception in V2X cooperative environments.

## 4 Experiments

### 4.1 Experiment Settings

#### 4.1.1 Datasets Configuration

Autonomous driving is a data-driven technology that requires large-scale and diverse datasets for model training and iterative refinement. However, the distribution of real-world driving data is inherently long-tailed: common scenarios

appear frequently, whereas safety-critical corner cases occur with extremely low probability. This challenge is further amplified when high-level driving functions are deployed only in geographically restricted areas, limiting exposure to rare yet crucial situations. Although current systems can perform reliably in relatively structured environments (e.g., highways), their performance in complex urban scenarios remains insufficient, primarily due to the lack of long-tail data. Achieving a safety level surpassing human drivers is estimated to require tens of billions of testing kilometers [32], making real-world data collection prohibitively expensive and time-consuming.

To comprehensively evaluate the proposed model under diverse conditions and cooperative paradigms, we employ a dataset suite covering both real-world and simulated V2X scenarios, including V2I and V2V collaboration:

- **Real-world evaluation:** V2X-Seq-SPD [5] is used to assess model performance under realistic traffic conditions, where inherent sensor noise and annotation inconsistencies provide a stringent test for practical robustness.
- **Simulation-based evaluation:** V2X-Sim-V2V and V2X-Sim-V2I, constructed from V2X-Sim [6], offer noise-free ground truth labels, enabling controlled analysis of model architecture, multi-view collaboration, and upper-bound performance without real-world artifacts.
- **Complementary collaboration paradigms:** V2I datasets (V2X-Seq-SPD, V2X-Sim-V2I) represent distributed and infrastructure-assisted perception, whereas V2V datasets (V2X-Sim-V2V) reflect fully distributed multi-agent collaboration. Together, they form a holistic benchmark for V2X collaborative perception.

All datasets are unified into the nuScenes format to standardize data loading and annotation structure. A consolidated dataset comparison is shown in Table 1.

Table 1: Comparison of Datasets

Attribute	V2X-Seq-SPD	V2X-Sim-V2V	V2X-Sim-V2I
collaboration Type	V2I	V2V	V2I
Modalities	Point cloud, Image	Point cloud, Image	Point cloud, Image
Ego Sensors	LiDAR, Camera	LiDAR, Camera	LiDAR, Camera
Other Sensors	LiDAR, Camera	LiDAR, Camera	LiDAR, Camera
Sampling Rate	10Hz	5Hz	5Hz
Total Scenes	67	36	65
Training Scenes	46	24	46
Test Scenes	21	12	19
Total Frames	10761	13600	6500
Training Frames	7445	2400	4600
Test Frames	3316	1200	1900
Ego Samples	149672	33671	64091
Other-agent Samples	199067	33389	110082
Cooperative Samples	281078	51172	108367

#### 4.1.2 Evaluation Metrics

We adopt mAP for 3D object detection accuracy, AMOTA for multi-object tracking performance, and AMOTP for tracking localization precision.

#### 4.1.3 Implementation Details of XET-V2X

The proposed XET-V2X framework is implemented under the Transformer architecture [33]. The model integrates multi-view features from both ego and cooperative agents, using synchronized LiDAR and image sequences for spatiotemporal 3D perception.

Point clouds are voxelized using a pillar-based representation with a voxel size of [0.2, 0.2, 8]. For the V2X-Seq-SPD dataset [5], the LiDAR range for CAVs is set to [-51.2, -51.2, -5.0, 51.2, 51.2, 3.0], while for RSUs it is set to [0, -51.2, -5.0, 102.4, 51.2, 3.0]. For the V2X-Sim-V2V and V2X-Sim-V2I datasets, the LiDAR range for both CAVs and RSUs is set to [-51.2, -51.2, -3.0, 51.2, 51.2, 5.0].

A PillarFeatureNet encodes per-pillar features (4-dimensional point attributes), followed by a SECOND backbone with layer configuration [3,5,5] and output channels [64,128,256]. The multi-scale LiDAR features are aggregated by an FPN into 256-dimensional representations.

Images are processed using a ResNet-101 backbone [29] with multi-scale feature extraction. The resulting feature maps are fused via an FPN into 256-dimensional outputs. Standard image normalization and GridMask augmentation are applied during training.

The temporal module consists of six encoder layers and six decoder layers. Each encoder layer includes temporal self-attention to model historical dependencies, followed by two-stage spatial cross-attention to fuse multimodal spatial features. The decoder adopts a dual-attention structure and supports 900 learnable object queries. The BEV feature map is configured to a resolution of  $200 \times 200$  with 256 channels.

A unified multi-task head performs 3D object detection and online tracking, employing a Hungarian assigner for bipartite matching. Focal Loss is used for classification, and L1 loss for bounding-box regression. The tracker incorporates both semantic consistency and geometric association. Supported categories include car, pedestrian, motorcycle, and bicycle.

Each input sequence contains five frames, with the first four serving as historical context. Training uses the AdamW optimizer with a learning rate of  $2 \times 10^{-4}$  and weight decay 0.01. A cosine annealing schedule with 500 warm-up iterations, 10 epochs, and gradient clipping (norm 35) is applied. During inference, the model outputs both detection and tracking predictions in a single forward pass.

#### 4.1.4 Baseline Model Configuration

To comprehensively evaluate the improvements brought by XET-V2X in end-to-end 3D spatiotemporal perception, the following baselines are adopted:

- **CET-V**: Employs only the ego-view monocular image stream and outputs detection and tracking results end-to-end. Represents a single-view, single-modality (image) end-to-end framework.
- **LET-V**: Uses only the ego-view narrow-FoV LiDAR, with end-to-end detection and tracking. Represents single-view, single-modality (LiDAR) end-to-end perception.
- **XET-V**: Uses both ego-view images and ego-view LiDAR as inputs, without cooperative viewpoints. Represents single-view, multimodal (image + LiDAR) end-to-end perception.
- **CET-V2X**: Incorporates ego-view images and multi-view camera images from cooperative agents, without using LiDAR. Represents multi-view cooperative, single-modality (image) end-to-end perception.
- **LET-V2X**: Incorporates ego-view LiDAR and multi-view LiDAR from cooperative agents, without using images. Represents multi-view cooperative, single-modality (LiDAR) end-to-end perception.

These baselines allow systematic assessment of XET-V2X in terms of perception accuracy, robustness, multi-view collaboration, and cross-agent feature fusion, as summarized in Table 2.

Table 2: Comparison of Different Baseline Models

Model	End-to-End	Multi-view	Multi-modal	Viewpoints		Modalities	
				Ego	Others	LiDAR	Image
CET-V	✓			✓			✓
LET-V	✓			✓		✓	
XET-V	✓		✓	✓	✓	✓	✓
LET-V2X	✓	✓		✓	✓	✓	
CET-V2X	✓	✓		✓	✓		✓

## 4.2 Quantitative Evaluation

### 4.2.1 Overall Performance

As reported in Table 3 and Figures 4, the XET family consistently achieves state-of-the-art accuracy on the real-world V2X-Seq-SPD dataset [5] and the simulated V2X-Sim-V2V/V2X-Sim-V2I benchmarks [6].

Across all datasets, XET-V outperforms LET-V and CET-V, while XET-V2X surpasses LET-V2X and CET-V2X in mAP, AMOTA, and AMOTP. Furthermore, XET-VIC exceeds XET, demonstrating that introducing multi-view collaboration on top of multi-modal fusion yields additional geometric complementarity and temporal robustness. These results indicate that the proposed end-to-end framework delivers stable gains in diverse environments and maintains strong generalization across real and synthetic domains.

Table 3: Performance comparison under different communication delay conditions on three V2X benchmarks. Latency is measured in frame-level delay. For V2X-Seq-SPD [5] (10 Hz), one frame corresponds to 100 ms, while for V2X-Sim-V2V and V2X-Sim-V2I (5 Hz), one frame corresponds to 200 ms.

Model	Latency (frames)	V2X-Seq-SPD			V2X-Sim-V2V			V2X-Sim-V2I		
		mAP↑	AMOTA↑	AMOTP↓	mAP↑	AMOTA↑	AMOTP↓	mAP↑	AMOTA↑	AMOTP↓
LET-V	-	0.449	0.437	1.175	0.424	0.315	1.401	0.379	0.308	1.432
CET-V	-	0.198	0.241	1.618	0.217	0.190	1.646	0.177	0.136	1.726
XET-V	-	0.490	0.469	1.122	0.510	0.459	1.168	0.412	0.364	1.335
LET-V2X	0	0.668	0.616	0.859	0.502	0.391	0.865	0.653	0.562	0.671
LET-V2X	1	0.608	0.592	0.951	0.462	0.373	0.898	0.573	0.511	0.817
LET-V2X	2	0.546	0.543	1.009	0.451	0.346	0.938	0.508	0.430	0.901
CET-V2X	0	0.179	0.169	1.630	0.313	0.291	1.419	0.714	0.782	0.567
CET-V2X	1	0.188	0.169	1.631	0.299	0.272	1.465	0.638	0.723	0.706
CET-V2X	2	0.187	0.169	1.633	0.278	0.240	1.499	0.572	0.626	0.826
<b>XET-V2X</b>	0	<b>0.795</b>	<b>0.787</b>	<b>0.591</b>	<b>0.766</b>	<b>0.731</b>	<b>0.677</b>	<b>0.858</b>	<b>0.819</b>	<b>0.476</b>
XET-V2X	1	<b>0.743</b>	<b>0.761</b>	<b>0.668</b>	<b>0.714</b>	<b>0.698</b>	<b>0.760</b>	<b>0.746</b>	<b>0.776</b>	<b>0.584</b>
XET-V2X	2	<b>0.688</b>	<b>0.722</b>	<b>0.730</b>	<b>0.668</b>	<b>0.652</b>	<b>0.804</b>	<b>0.664</b>	<b>0.668</b>	<b>0.712</b>

#### 4.2.2 Quantitative Analysis of Multi-View Collaboration

The V2X-Seq-SPD dataset [5] provides a realistic vehicle–infrastructure cooperative perception benchmark, where both vehicle-side and infrastructure-side nodes are equipped with a forward-facing camera and LiDAR. Compared with synthetic datasets, V2X-Seq-SPD features challenging illumination variations, frequent occlusions, and irregular traffic behaviors. In this scenario, the elevated infrastructure viewpoint effectively complements vehicle-side blind spots. As reported in Table 3 and Fig. 4a–Fig. 4c, XET-V2X consistently outperforms the single-vehicle baseline XET-V under all latency settings. Under zero latency, XET-V2X achieves mAP and AMOTA improvements of 30.5% and 31.8%, respectively, while also reducing AMOTP. Performance gains remain stable under increasing V2I delays, indicating strong robustness to communication latency in real-world environments.

The V2X-Sim-V2V scenario [6] evaluates multi-vehicle collaboration with distinct characteristics from vehicle–infrastructure settings. Although constrained by motion consistency and temporal alignment, V2V collaboration provides dense neighboring viewpoints in non-intersection road segments, forming a dynamic surround-view perception structure. As shown in Table 3 and Fig. 4d–Fig. 4f, XET-V2X surpasses XET-V across all evaluated delays. At zero latency, mAP and AMOTA increase by 25.6% and 27.2%, demonstrating effective exploitation of complementary vehicle viewpoints. Notable performance advantages are preserved even under large communication delays, highlighting robustness under sparse and asynchronous collaboration.

In the V2X-Sim-V2I scenario [6], performance gains primarily stem from complementary sensing perspectives. The infrastructure node, equipped with a 360° LiDAR and multi-camera setup, provides comprehensive coverage of intersections and long-range road segments, compensating for the limited forward-facing vehicle view. As illustrated in Table 3 and Fig. 4g–Fig. 4i, XET-V2X achieves substantial improvements over XET-V, with mAP and AMOTA gains of 44.6% and 45.5% under zero latency. Consistent advantages under delayed communication further confirm the effectiveness of vehicle–infrastructure collaboration.

Across both real-world and simulated datasets, multi-view collaboration yields consistent and significant performance gains over single-vehicle perception. These results demonstrate that the proposed XET-V2X framework effectively leverages complementary viewpoints and maintains robustness under varying communication latency.

#### 4.2.3 Quantitative Analysis of Multi-Modal Fusion

Results on the real-world V2X-Seq-SPD dataset [5], summarized in Table 3 and Fig. 4a–Fig. 4c, evaluate the effectiveness of multimodal fusion from both single-vehicle and multi-view cooperative perspectives. For single-vehicle perception, XET-V, which fuses image and point cloud modalities, consistently outperforms the unimodal baselines LET-V (LiDAR-only) and CET-V (camera-only). XET-V improves mAP and AMOTA over LET-V by 4.1% and 3.2%, and outperforms CET-V by 29.2% and 22.8%, respectively, with consistent AMOTP reductions. These results indicate that multimodal fusion provides complementary geometric and semantic cues even under a single-view setting. For multi-view cooperative perception, XET-V2X further amplifies the benefits of multimodal fusion. Under ideal communication conditions, XET-V2X outperforms LET-V2X by 12.7% in mAP and 17.1% in AMOTA, and surpasses

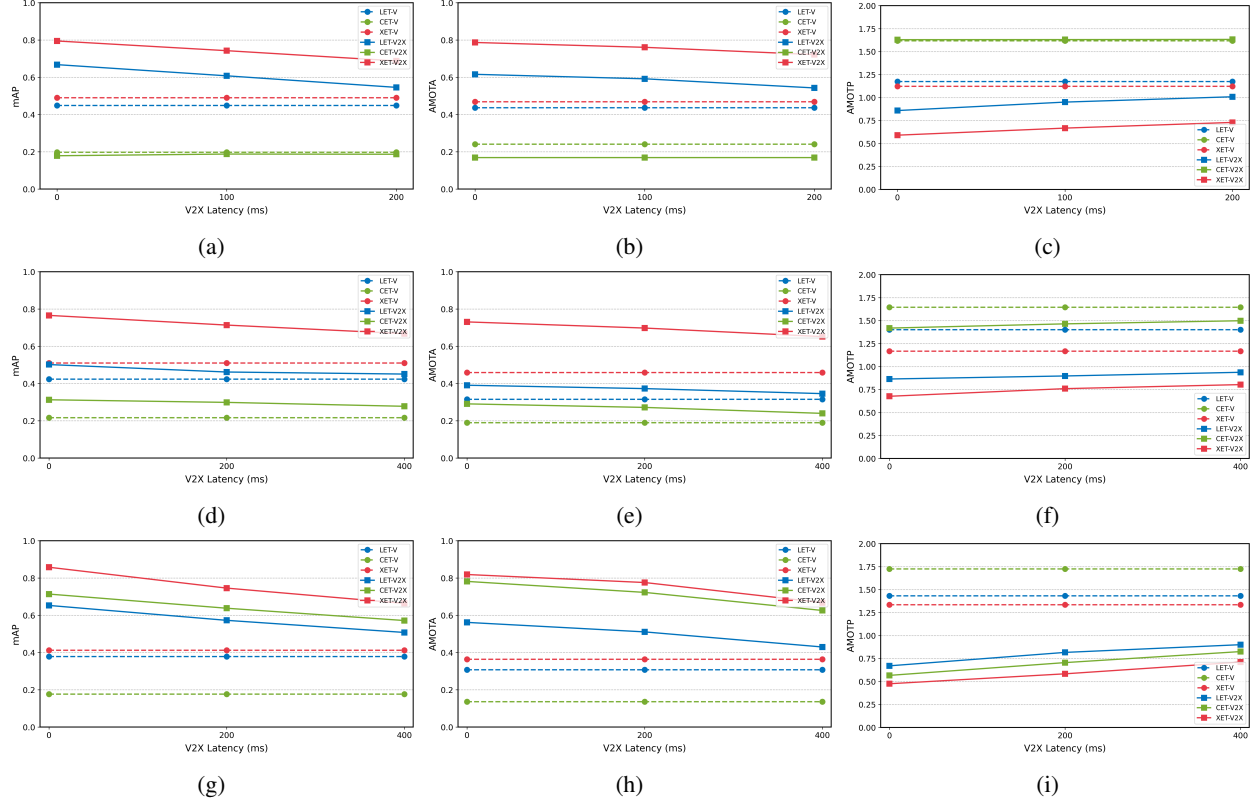


Figure 4: Performance comparison under different communication latency conditions across three datasets. Subfigures show: (a) V2X-Seq-SPD dataset detection performance (mAP) [5]; (b) V2X-Seq-SPD dataset tracking performance (AMOTA) [5]; (c) V2X-Seq-SPD dataset tracking performance (AMOTP) [5]; (d) V2X-Sim-V2V dataset detection performance (mAP) [6]; (e) V2X-Sim-V2V dataset tracking performance (AMOTA) [6]; (f) V2X-Sim-V2V dataset tracking performance (AMOTP) [6]; (g) V2X-Sim-V2I dataset detection performance (mAP) [6]; (h) V2X-Sim-V2I dataset tracking performance (AMOTA) [6]; (i) V2X-Sim-V2I dataset tracking performance (AMOTP) [6].

CET-V2X by 61.6% and 61.8%, respectively, with a clear reduction in AMOTP. Although V2X-Seq-SPD exhibits annotation projection errors between point clouds and images, leading to feature misalignment during fusion, XET-V2X still delivers stable and significant gains, demonstrating strong robustness in real-world environments.

Similar observations are obtained on the simulated V2X-Sim-V2V dataset [6], as shown in Table 3 and Fig. 4d–Fig. 4f. In the single-vehicle setting, XET-V consistently outperforms LET-V and CET-V, confirming the effectiveness of multimodal fusion without collaboration. In the cooperative setting, XET-V2X achieves the best performance across all delay conditions. At zero latency, XET-V2X improves mAP and AMOTA by 26.4% and 34.0% over LET-V2X, and by 45.3% and 44.0% over CET-V2X. Performance advantages remain evident under increasing communication delays, indicating that multimodal fusion effectively mitigates the impact of latency and dynamic misalignment in V2V collaboration.

Consistent trends are also observed on the V2X-Sim-V2I dataset [6], as reported in Table 3 and Fig. 4g–Fig. 4i. In the single-vehicle setting, XET-V achieves moderate but consistent improvements over LET-V and more pronounced gains over CET-V. This behavior is mainly attributed to the limited overlap between the vehicle perception region and the dataset ground truth, where monocular perception can already achieve reasonable performance. In contrast, camera-only methods remain constrained by depth ambiguity, which is effectively compensated by multimodal fusion. In the vehicle–infrastructure cooperative setting, XET-V2X again achieves the strongest results. Under zero latency, XET-V2X improves mAP and AMOTA over LET-V2X by 20.5% and 25.7%, respectively, while maintaining consistent advantages over CET-V2X. These results highlight the additive benefits of combining multimodal fusion with multi-view collaboration.

Across both real-world and simulated datasets, multimodal fusion consistently outperforms unimodal perception in single-vehicle scenarios and yields even larger gains under multi-view cooperation. This demonstrates that image and

point cloud modalities are highly complementary, and that their fusion enables more accurate and robust 3D temporal perception, particularly under ideal communication conditions.

#### 4.2.4 Ablation Study on Multimodal Fusion Design

Table 4: Performance comparison under different fusion orders on three V2X benchmarks. Fusion Order denotes the feature refinement order in cross-modal attention:  $\checkmark$  for Image  $\rightarrow$  Point Cloud, blank for Point Cloud  $\rightarrow$  Image.

Model	Fusion	V2X-Seq-SPD			V2X-Sim-V2V			V2X-Sim-V2I		
		Order	mAP $\uparrow$	AMOTA $\uparrow$	AMOTP $\downarrow$	mAP $\uparrow$	AMOTA $\uparrow$	AMOTP $\downarrow$	mAP $\uparrow$	AMOTA $\uparrow$
XET-V	$\checkmark$	0.456	0.421	1.235	0.495	0.454	1.180	0.399	0.358	1.350
		0.490	0.469	1.122	0.510	0.459	1.168	0.412	0.364	1.335
XET-V2X	$\checkmark$	0.707	0.663	0.823	0.735	0.700	0.748	0.797	0.813	0.508
		<b>0.795</b>	<b>0.787</b>	<b>0.591</b>	<b>0.766</b>	<b>0.731</b>	<b>0.677</b>	<b>0.858</b>	<b>0.819</b>	<b>0.476</b>

This ablation study investigates the design choices of the proposed multimodal fusion module, with particular emphasis on the contribution of multimodal interaction and the feature fusion order within the V2X spatial cross-attention layers. Quantitative comparisons are reported on three representative V2X benchmarks, including a real-world sequential dataset and two simulated cooperative perception settings.

**Effect of Fusion Order.** To further analyze the robustness of the proposed fusion design, we evaluate two alternative feature fusion orders within the stacked V2X spatial cross-attention layers: (i) point cloud features refined by image features (Point  $\rightarrow$  Image), and (ii) image features refined by point cloud features (Image  $\rightarrow$  Point). As shown in Table 4, both fusion orders consistently outperform single-modality and single-view baselines, suggesting that the cross-attention-based fusion mechanism is not sensitive to a specific interaction sequence.

Nevertheless, the Image  $\rightarrow$  Point fusion order exhibits slightly superior and more stable performance across all benchmarks. In particular, XET-V2X with Image  $\rightarrow$  Point fusion achieves the highest mAP and AMOTA on all three datasets, while also yielding lower AMOTP values, indicating more precise localization. This trend is consistent across both real-world and simulated scenarios, suggesting that refining image features first provides more informative semantic guidance for subsequent point cloud feature enhancement.

Based on these observations, the Image  $\rightarrow$  Point fusion order is adopted in the final model. The ablation results indicate that the performance gains of XET primarily stem from effective cross-modal and cross-view interaction, while the selected fusion order further improves accuracy and robustness in V2X cooperative perception scenarios.

#### 4.2.5 Qualitative Visualization Results

To complement the quantitative evaluation, we present qualitative visualization results to further analyze the perception behavior of the proposed models under diverse V2X scenarios. Representative inference results on the V2X-Seq-SPD [5], V2X-Sim-V2V, and V2X-Sim-V2I [6] benchmarks are illustrated. Due to space limitations, only selected examples are shown in the main paper, while additional qualitative visualizations are provided in the Appendix, as illustrated in Fig. 6.

Fig. 5 presents a representative qualitative comparison on the real-world V2X-Seq-SPD benchmark, illustrating the differences between single-vehicle and cooperative perception, as well as between unimodal and multimodal designs. The visualizations compare predicted 3D detection and tracking results with ground-truth annotations. Consistent colors across frames indicate the same tracked object over time, enabling intuitive assessment of detection completeness and temporal continuity. Semi-transparent dashed boxes indicate false negatives (missed detections), while semi-transparent dashed circles denote false positives, providing visual cues for analyzing failure cases under occlusion, dense traffic, and long-term tracking conditions.

**Single-Vehicle vs. Cooperative Perception.** Across all datasets, single-vehicle models exhibit noticeable limitations, particularly in scenarios involving occlusions or limited fields of view. Missed detections and fragmented trajectories are frequently observed, especially in crowded or dynamically changing environments. In contrast, V2X-based cooperative models significantly alleviate these issues by leveraging complementary viewpoints from multiple agents, resulting in more complete detections and smoother temporal associations.

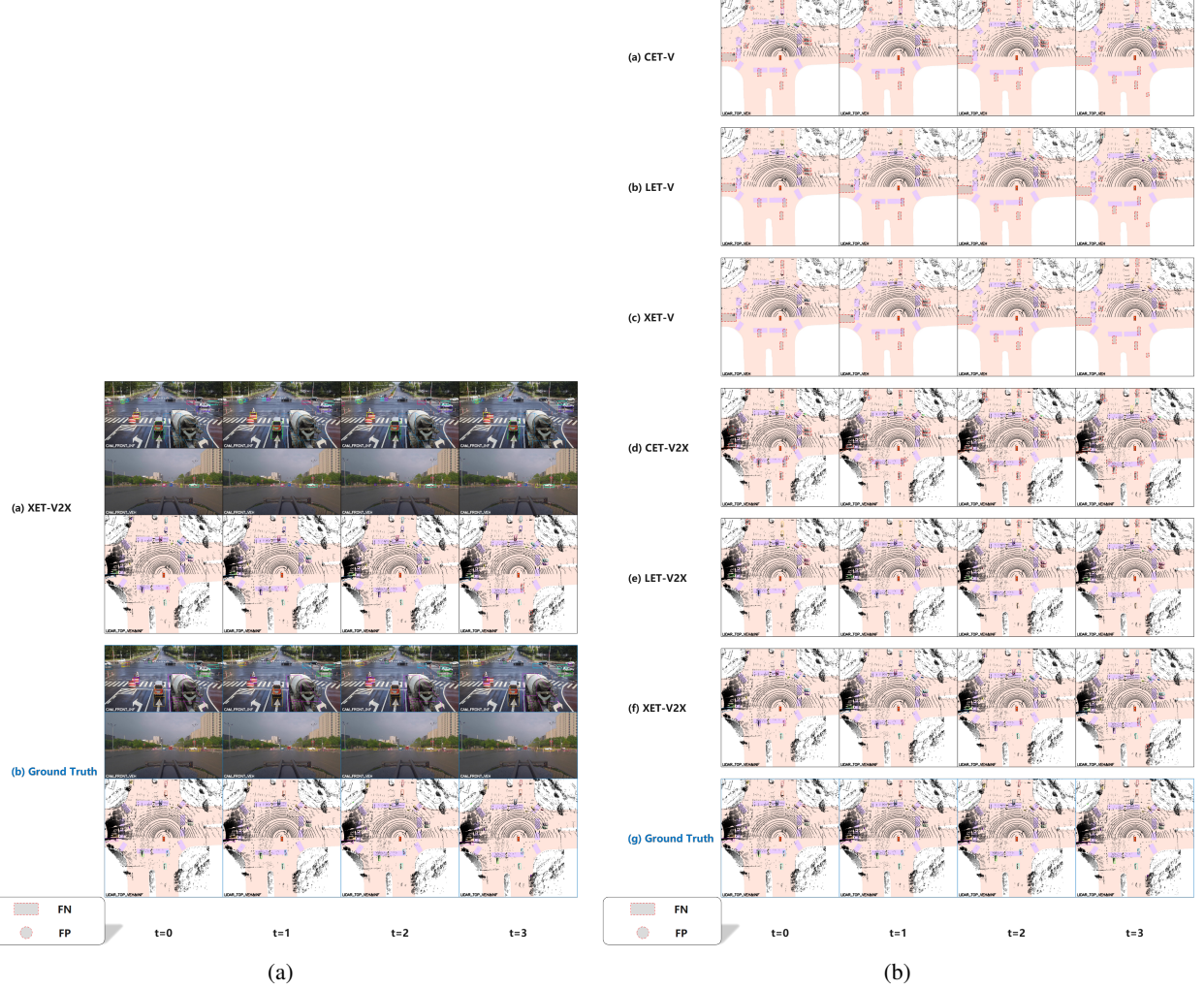


Figure 5: Qualitative visualization and comparison of perception results on the V2X-Seq-SPD dataset [5]. (a) Qualitative visualization of XET-V2X results. (b) Qualitative comparison of different perception models.

**Effectiveness of Multimodal and Multi-View Fusion.** Among all evaluated methods, XET-V2X consistently demonstrates the most robust qualitative performance. On the real-world V2X-Seq-SPD dataset, XET-V2X produces fewer missed detections and maintains stable object identities over long temporal spans. Similar trends are observed in the simulated V2X-Sim-V2V and V2X-Sim-V2I benchmarks, where XET-V2X effectively recovers targets located in blind regions and preserves trajectory continuity in dense multi-agent interactions. These results visually confirm the quantitative gains reported earlier, highlighting the complementary benefits of multimodal feature fusion and multi-view collaboration in complex V2X perception scenarios.

The qualitative results indicate that the proposed XET-V2X framework not only improves detection accuracy but also enhances temporal consistency and robustness, particularly under challenging conditions involving occlusions, dense traffic, and extended temporal tracking.

## 5 Conclusion

This work presents XET-V2X, an end-to-end spatiotemporal perception framework designed for multi-view cooperative and multimodal fusion in V2X environments. By jointly modeling temporal dynamics, cross-view collaboration, and multimodal feature interactions, the proposed approach effectively addresses the performance degradation commonly observed in single-view or single-modality perception systems under occlusions, limited fields of view, and calibration uncertainties.

Comprehensive experiments on V2X-Seq-SPD [5], V2X-Sim-V2I, and V2X-Sim-V2V [6] demonstrate the effectiveness of the proposed framework from both quantitative and qualitative perspectives. Quantitative results confirm that multi-view collaboration and multimodal fusion each contribute substantial performance gains in detection and tracking, while their unified integration within XET-VIC consistently achieves the best overall performance across all benchmarks. Ablation studies further verify that the proposed cross-modal fusion design provides robust and stable improvements regardless of feature extraction order.

Qualitative visualizations offer intuitive evidence supporting the quantitative findings. Single-vehicle models frequently suffer from missed detections and unstable temporal associations in complex traffic scenarios, whereas cooperative models significantly alleviate these issues. In particular, XET-V2X/XET-V2V exhibits the fewest missed targets and the most consistent long-term tracking, highlighting the complementary advantages of multi-view collaboration and multimodal fusion.

Overall, the proposed XET-VIC framework demonstrates strong robustness and generalization capability under both real-world and simulated V2X settings, making it a promising solution for scalable and reliable cooperative spatiotemporal perception in autonomous driving systems.

## A Qualitative Visualization on V2X-Sim Datasets

This section presents qualitative visualization results on the V2X-Sim-V2V and V2X-Sim-V2I datasets [6]. Predicted 3D detection and tracking results are compared with ground-truth annotations. Consistent colors indicate the same tracked objects across time. Semi-transparent dashed boxes denote false negatives (missed detections), while semi-transparent dashed circles indicate false positives.

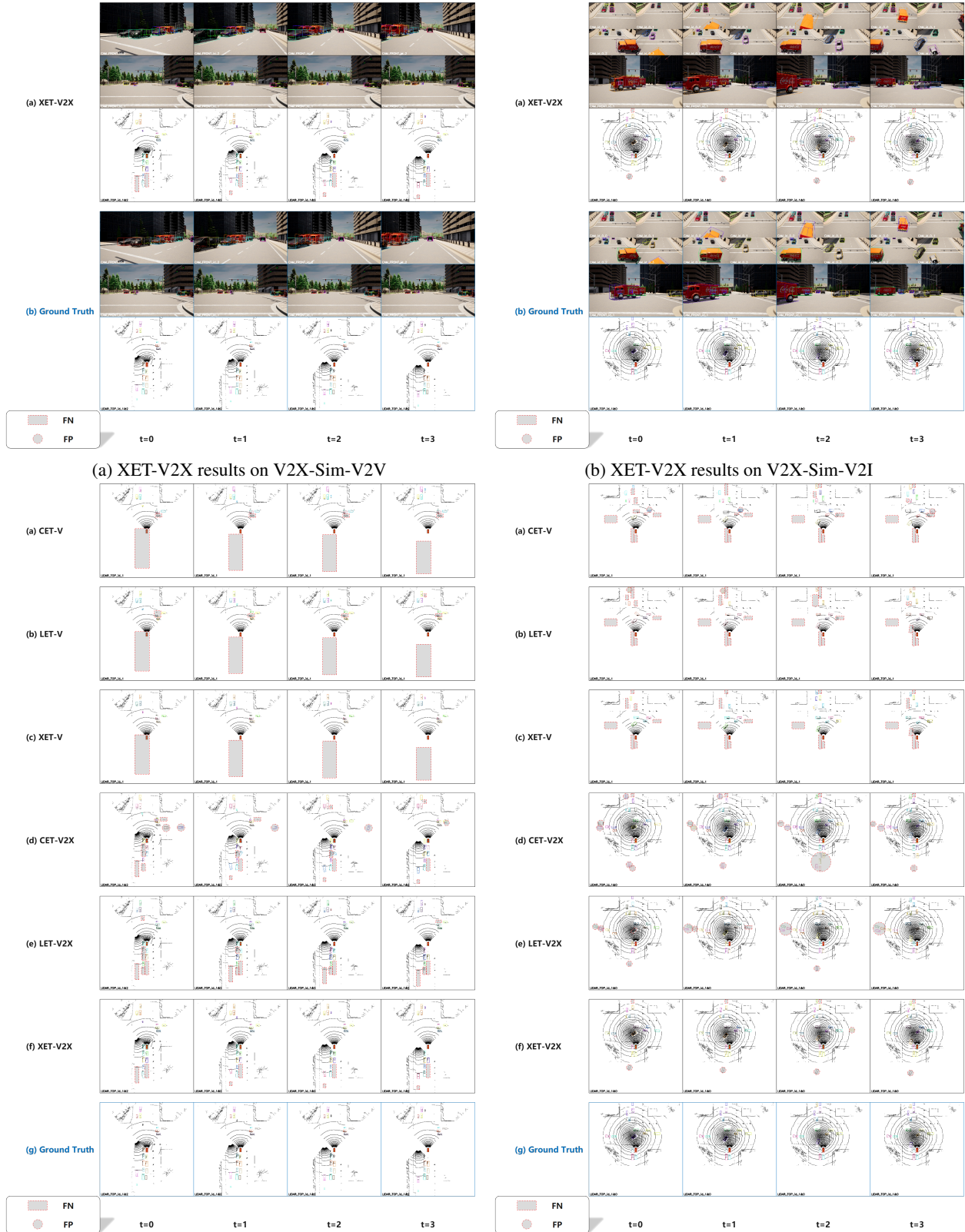


Figure 6: Qualitative visualization and comparison of perception results on the V2X-Sim datasets [6].

## References

- [1] Qi Chen, Sihai Tang, Qing Yang, and Song Fu. Cooper: Cooperative perception for connected autonomous vehicles based on 3d point clouds. In *2019 IEEE 39th International Conference on Distributed Computing Systems (ICDCS)*, pages 514–524. IEEE, 2019.
- [2] Qi Chen, Xu Ma, Sihai Tang, Jingda Guo, Qing Yang, and Song Fu. F-cooper: Feature based cooperative perception for autonomous vehicle edge computing system using 3d point clouds. In *Proceedings of the 4th ACM/IEEE Symposium on Edge Computing*, pages 88–100, 2019.
- [3] Tsun-Hsuan Wang, Sivabalan Manivasagam, Ming Liang, Bin Yang, Wenyuan Zeng, and Raquel Urtasun. V2vnet: Vehicle-to-vehicle communication for joint perception and prediction. In *Computer Vision–ECCV 2020: 16th European Conference, Glasgow, UK, August 23–28, 2020, Proceedings, Part II 16*, pages 605–621. Springer, 2020.
- [4] Yue Hu, Shaoheng Fang, Zixing Lei, Yiqi Zhong, and Siheng Chen. Where2comm: Communication-efficient collaborative perception via spatial confidence maps. *Advances in neural information processing systems*, 35:4874–4886, 2022.
- [5] Haibao Yu, Wenxian Yang, Hongzhi Ruan, Zhenwei Yang, Yingjuan Tang, Xu Gao, Xin Hao, Yifeng Shi, Yifeng Pan, Ning Sun, et al. V2x-seq: A large-scale sequential dataset for vehicle-infrastructure cooperative perception and forecasting. In *Proceedings of the IEEE/CVF Conference on Computer Vision and Pattern Recognition*, pages 5486–5495, 2023.
- [6] Yiming Li, Dekun Ma, Ziyan An, Zixun Wang, Yiqi Zhong, Siheng Chen, and Chen Feng. V2x-sim: Multi-agent collaborative perception dataset and benchmark for autonomous driving. *IEEE Robotics and Automation Letters*, 7(4):10914–10921, 2022.
- [7] Runsheng Xu, Xin Xia, Jinlong Li, Hanzhao Li, Shuo Zhang, Zhengzhong Tu, Zonglin Meng, Hao Xiang, Xiaoyu Dong, Rui Song, et al. V2v4real: A real-world large-scale dataset for vehicle-to-vehicle cooperative perception. In *Proceedings of the IEEE/CVF Conference on Computer Vision and Pattern Recognition*, pages 13712–13722, 2023.
- [8] Florian Seeliger, Galia Weidl, Dominik Petrich, Frederik Naujoks, Gabi Breuel, Alexandra Neukum, and Klaus Dietmayer. Advisory warnings based on cooperative perception. In *2014 IEEE Intelligent Vehicles Symposium Proceedings*, pages 246–252. IEEE, 2014.
- [9] Yeojun Kim, Luca Onesto, Samuel Tay, Lujie Yang, Jacopo Guanetti, Sergio Savaresi, and Francesco Borrelli. Shared perception for connected and automated vehicles. In *2020 IEEE Intelligent Vehicles Symposium (IV)*, pages 21–26. IEEE, 2020.
- [10] Zhenwei Yang, Jilei Mao, Wenxian Yang, Yibo Ai, Yu Kong, Haibao Yu, and Weidong Zhang. Lidar-based end-to-end temporal perception for vehicle-infrastructure cooperation. *IEEE INTERNET OF THINGS JOURNAL*, 12(13):22862–22874, JUL 1 2025.
- [11] Haibao Yu, Yizhen Luo, Mao Shu, Yiyi Huo, Zebang Yang, Yifeng Shi, Zhenglong Guo, Hanyu Li, Xing Hu, Jirui Yuan, et al. Dair-v2x: A large-scale dataset for vehicle-infrastructure cooperative 3d object detection. In *Proceedings of the IEEE/CVF Conference on Computer Vision and Pattern Recognition*, pages 21361–21370, 2022.
- [12] Runsheng Xu, Hao Xiang, Xin Xia, Xu Han, Jinlong Li, and Jiaqi Ma. Opv2v: An open benchmark dataset and fusion pipeline for perception with vehicle-to-vehicle communication. In *2022 International Conference on Robotics and Automation (ICRA)*, pages 2583–2589. IEEE, 2022.
- [13] Sourabh Vora, Alex H Lang, Bassam Helou, and Oscar Beijbom. Pointpainting: Sequential fusion for 3d object detection. In *Proceedings of the IEEE/CVF conference on computer vision and pattern recognition*, pages 4604–4612, 2020.
- [14] Ramin Nabati and Hairong Qi. Centerfusion: Center-based radar and camera fusion for 3d object detection. In *Proceedings of the IEEE/CVF Winter Conference on Applications of Computer Vision*, pages 1527–1536, 2021.
- [15] Zehui Chen, Zhenyu Li, Shiquan Zhang, Liangji Fang, Qinhong Jiang, and Feng Zhao. Deformable feature aggregation for dynamic multi-modal 3d object detection. In *European conference on computer vision*, pages 628–644. Springer, 2022.
- [16] Yingwei Li, Adams Wei Yu, Tianjian Meng, Ben Caine, Jiquan Ngiam, Daiyi Peng, Junyang Shen, Yifeng Lu, Denny Zhou, Quoc V Le, et al. Deepfusion: Lidar-camera deep fusion for multi-modal 3d object detection. In *Proceedings of the IEEE/CVF conference on computer vision and pattern recognition*, pages 17182–17191, 2022.

- [17] Xuyang Bai, Zeyu Hu, Xinge Zhu, Qingqiu Huang, Yilun Chen, Hongbo Fu, and Chiew-Lan Tai. Transfusion: Robust lidar-camera fusion for 3d object detection with transformers. In *Proceedings of the IEEE/CVF conference on computer vision and pattern recognition*, pages 1090–1099, 2022.
- [18] Xuanyao Chen, Tianyuan Zhang, Yue Wang, Yilun Wang, and Hang Zhao. Futr3d: A unified sensor fusion framework for 3d detection. In *proceedings of the IEEE/CVF conference on computer vision and pattern recognition*, pages 172–181, 2023.
- [19] Zeyu Yang, Jiaqi Chen, Zhenwei Miao, Wei Li, Xiatian Zhu, and Li Zhang. Deepinteraction: 3d object detection via modality interaction. *Advances in Neural Information Processing Systems*, 35:1992–2005, 2022.
- [20] AJ Piergiovanni, Vincent Casser, Michael S Ryoo, and Anelia Angelova. 4d-net for learned multi-modal alignment. In *Proceedings of the IEEE/CVF International Conference on Computer Vision*, pages 15435–15445, 2021.
- [21] Ming Chang, Xishan Zhang, Rui Zhang, Zhipeng Zhao, Guanhua He, and Shaoli Liu. Recurrentbev: A long-term temporal fusion framework for multi-view 3d detection. In *European Conference on Computer Vision*, pages 131–147. Springer, 2024.
- [22] Zewei Zhou, Hao Xiang, Zhaoliang Zheng, Seth Z Zhao, Mingyue Lei, Yun Zhang, Tianhui Cai, Xinyi Liu, Johnson Liu, Maheswari Bajji, et al. V2xpnp: Vehicle-to-everything spatio-temporal fusion for multi-agent perception and prediction. *arXiv preprint arXiv:2412.01812*, 2024.
- [23] Tianwei Yin, Xingyi Zhou, and Philipp Krahenbuhl. Center-based 3d object detection and tracking. In *Proceedings of the IEEE/CVF conference on computer vision and pattern recognition*, pages 11784–11793, 2021.
- [24] Tim Meinhardt, Alexander Kirillov, Laura Leal-Taixe, and Christoph Feichtenhofer. Trackformer: Multi-object tracking with transformers. In *Proceedings of the IEEE/CVF conference on computer vision and pattern recognition*, pages 8844–8854, 2022.
- [25] Fangao Zeng, Bin Dong, Yuang Zhang, Tiancai Wang, Xiangyu Zhang, and Yichen Wei. Motr: End-to-end multiple-object tracking with transformer. In *European Conference on Computer Vision*, pages 659–675. Springer, 2022.
- [26] Jan-Nico Zaech, Alexander Liniger, Dengxin Dai, Martin Danelljan, and Luc Van Gool. Learnable online graph representations for 3d multi-object tracking. *IEEE Robotics and Automation Letters*, 7(2):5103–5110, 2022.
- [27] Ce Zhang, Chengjie Zhang, Yiluan Guo, Lingji Chen, and Michael Happold. Motiontrack: end-to-end transformer-based multi-object tracking with lidar-camera fusion. In *Proceedings of the IEEE/CVF Conference on Computer Vision and Pattern Recognition*, pages 151–160, 2023.
- [28] Alex H Lang, Sourabh Vora, Holger Caesar, Lubing Zhou, Jiong Yang, and Oscar Beijbom. Pointpillars: Fast encoders for object detection from point clouds. In *Proceedings of the IEEE/CVF conference on computer vision and pattern recognition*, pages 12697–12705, 2019.
- [29] Kaiming He, Xiangyu Zhang, Shaoqing Ren, and Jian Sun. Deep residual learning for image recognition. In *Proceedings of the IEEE conference on computer vision and pattern recognition*, pages 770–778, 2016.
- [30] Siqi Fan, Haibao Yu, Wenxian Yang, Jirui Yuan, and Zaiqing Nie. Quest: Query stream for vehicle-infrastructure cooperative perception. *arXiv preprint arXiv:2308.01804*, 2023.
- [31] Ziming Chen, Yifeng Shi, and Jinrang Jia. Transiff: An instance-level feature fusion framework for vehicle-infrastructure cooperative 3d detection with transformers. In *Proceedings of the IEEE/CVF International Conference on Computer Vision*, pages 18205–18214, 2023.
- [32] Shuo Feng, Haowei Sun, Xintao Yan, Haojie Zhu, Zhengxia Zou, Shengyin Shen, and Henry X Liu. Dense reinforcement learning for safety validation of autonomous vehicles. *Nature*, 615(7953):620–627, 2023.
- [33] Ashish Vaswani, Noam Shazeer, Niki Parmar, Jakob Uszkoreit, Llion Jones, Aidan N Gomez, Łukasz Kaiser, and Illia Polosukhin. Attention is all you need. *Advances in neural information processing systems*, 30, 2017.